ES

. Delin, R. Knighton, D. Clay, and
sand plains Management System
ultural research to protect water
neapolis, MN. Soil Water Cons.

K. Frank. 1993. Soil properties
il Sci. Soc. Am. J. 57:235–239.
l M.A. Hussey. 1987. Drought-
r-infrared aerial photography and
otogram. Eng. Rem. Sens. 53:

C. Rao. 1990. Spatial variability
la flatwoods site. Soil Sci. Soc.

er. 1990. Close-interval spatial
st central Texas. Soil Sci. Soc.

, J.A. Lamb, J.L. Anderson, and
gricultural chemicals in ground
gement System Evaluation Area.
h to Protect Water Quality,
MN. Soil Water Cons. Soc.

of soil variability with repetitive
J. 40:553–557.
1991. Digital terrain modeling:
ical, and biological applications.

A. Peterson. 1993. Soil attribute
i. Soc. Am. J. 57:443–452.
itions at the field level for soil
72.
models and soil formation: I.
i. 9(4):551–560.
U.S. Dep. Agric. Handb. No, 18.

Daniels, L.A Nelson, and H.J.
l landscape position on the
Soc. Am. J. 49:987–991.
rared linear combinations for
v. 8:127–150.
n of soil patterns and field soil
digital processing of aerial

20 Sensitivity Of Computed Terrain Attributes To The Number And Pattern Of GPS-Derived Elevation Data

Damian J. Spangrud
John P. Wilson

Department of Earth Sciences
Montana State University
Bozeman, Montana

Gerald A. Nielsen
Jeffrey S. Jacobsen

Department of Plant and Soil Science
Montana State University
Bozeman, Montana

David A. Tyler

Department of Survey Engineering
University of Maine
Orono, Maine

Soil specific crop management requires precise knowledge of soil properties and soil-landscape processes (Bouma & Finke, 1993; Burrough, 1993; Larson & Robert, 1993; Mulla, 1993). Detailed soil maps at scales of 1:6000 or 1:8000 and spatially variable soil attribute data are needed to guide soil specific crop management in most landscapes (Moore et al., 1993a). Conventional soil survey maps, however, are produced at scales of 1:15,000 and larger and as such, these maps seldom delineate all of a field's variability (Fisher, 1991). Similarly, the range of soil attribute values reported for most mapping units is sufficiently large that these data cannot adequately represent soil attribute variation (Moore et al., 1993a).

Soil scientists have proposed a variety of pedotransfer (regression) and other geostatistical functions which use soil texture, organic matter, soil structure, and bulk density input data as cost-effective alternatives to expensive soil attribute data collection efforts during the past decade (e.g., Rawls et al., 1982; Mulla, 1991; Wagenet et al., 1991). Other groups have used terrain

attributes derived from digital elevation models (DEMs) for this purpose. Klingebiel et al. (1987), for example, used slope, aspect, and elevation to increase the accuracy of mapped soil unit boundaries and thereby limit the within-unit variability, whereas Odeh et al. (1991) and Moore et al. (1993a, 1993b) have taken a slightly different approach and correlated soil properties with simple to measure primary and secondary terrain attributes that have physical meaning in an effort to improve soil attribute prediction.

Primary terrain attributes are calculated directly from elevation data and include variables such as slope gradient, aspect, specific catchment area, flowpath length, plan and profile curvature (Moore et al., 1991). Secondary attributes combine two or more primary attributes and are often used to characterize the spatial variability of specific processes occurring in the landscape. Moore et al. (1993a), for example, defined three compound indices (a wetness index, ω; a stream power index, Ω; and a sediment transport index, τ) and described their potential use in predicting the spatial distribution of soil properties as an aid to soil specific crop management.

These primary and secondary terrain attributes are usually computed from DEMs. A DEM is an ordered array of numbers that represents the spatial distribution of elevations above some arbitrary datum in a landscape. Moore et al. (1993a) review the various sources of DEMs and note that Global Positioning System (GPS) technology provides a rapid and relatively inexpensive way of obtaining data for the development of DEMs. This new technology offers important advantages in terms of scale and accuracy for soil specific farming applications given that the traditional sources of elevation data (e.g., 1:24000-scale USGS contour maps) and the 30 m DEMs derived from them with Z values rounded to the nearest meter offer data at too coarse a resolution for most site-specific farming applications. There is now a total of 24 GPS satellites in orbit and 5–10 of these satellites are visible to a receiver at any one time. A stationary receiver used in conjunction with a mobile receiver (in differential or kinematic mode) may provide X,Y,Z measurements down to centimeter accuracy (Tyler, 1993). The GPS operator determines the number and pattern (spread) of elevation data collected. Our research objective was to assess the impact of varying the number and pattern of GPS data on computed topographic attributes for a farm field in Montana.

METHODS AND DATA SOURCES

Elevation Data

Elevation data were collected at 6,284 different locations in 1991 with an Ashtech Sensor GPS receiver mounted on a pickup truck and an Ashtech P-12 GPS receiver operating in kinematic mode as part of a larger study examining potential nitrate contamination of ground water (Fig. 20–1a). These elevation data were converted to a regular 10 m grid with ANUDEM (Hutchinson, 1989) for subsequent analysis and display. This program takes irregular point or contour data and creates grid-based DEMs. ANUDEM automatically removes the spurious pits within user-defined tolerances, calculates stream lines and ridge lines

odels (DEMs) for this purpose.
slope, aspect, and elevation to
oundaries and thereby limit the
(1991) and Moore et al. (1993a,
ch and correlated soil properties
dary terrain attributes that have
attribute prediction.
directly from elevation data and
spect, specific catchment area,
Moore et al., 1991). Secondary
tributes and are often used to
fic processes occurring in the
defined three compound indices
and a sediment transport index,
ng the spatial distribution of soil
gement.
butes are usually computed from
bers that represents the spatial
datum in a landscape. Moore et
and note that Global Positioning
l relatively inexpensive way of
. This new technology offers
curacy for soil specific farming
f elevation data (e.g., 1:24000-
Ms derived from them with Z
too coarse a resolution for most
a total of 24 GPS satellites in
a receiver at any one time. A
obile receiver (in differential or
nts down to centimeter accuracy
number and pattern (spread) of
e was to assess the impact of
omputed topographic attributes

OURCES

erent locations in 1991 with an
up truck and an Ashtech P–12
t of a larger study examining
Fig. 20–1a). These elevation
ANUDEM (Hutchinson, 1989)
gram takes irregular point or
EM automatically removes the
tes stream lines and ridge lines

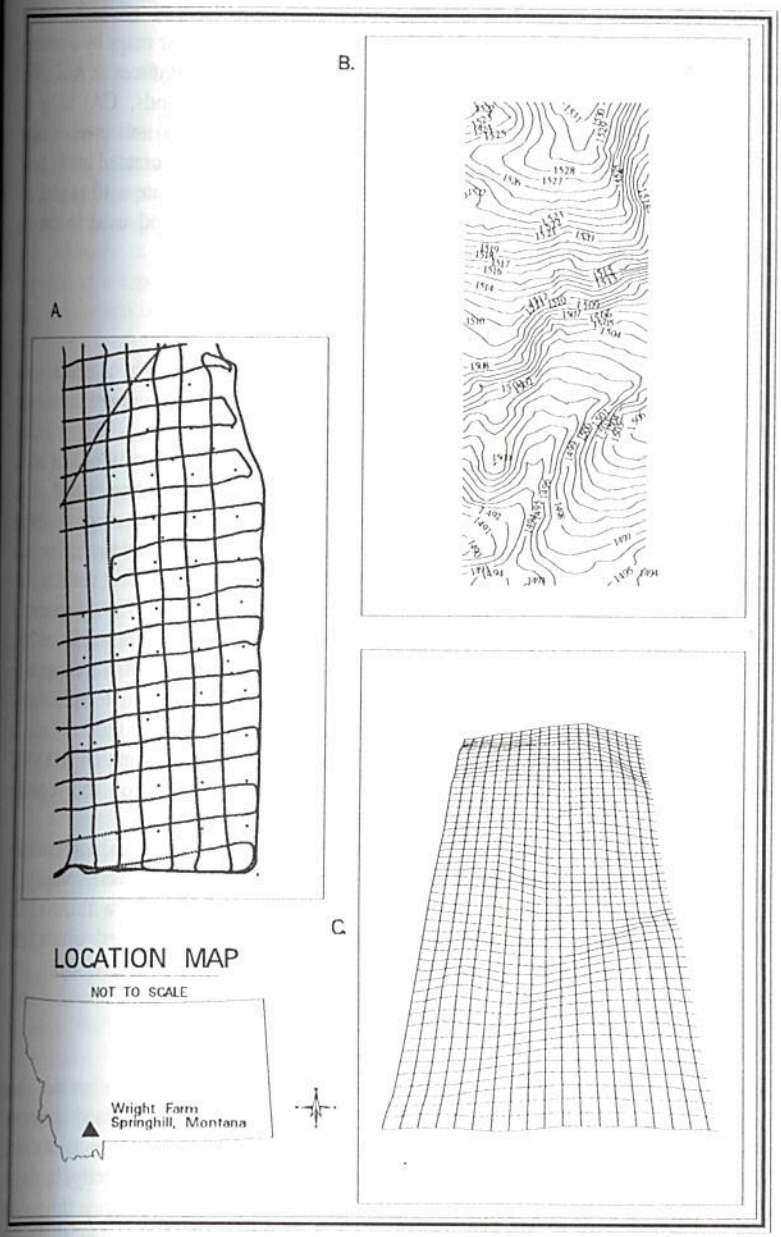

Fig. 20–1. Full GPS data set (a), contour map (b), and three-dimensional wire mesh diagram (c) for study area. Fig. 20–1 represents 6,284 X,Y,Z values obtained with a truck-mounted GPS receiver.

from points of locally maximum curvature on contour lines, and (most importantly) incorporates a drainage enforcement algorithm to maintain fidelity with a catchment's drainage network (Hutchinson, 1989; Moore et al., 1993d).

The 10 m DEMs were later converted to 1 m contour maps by converting the ANUDEM ASCII files consisting of X,Y,Z values to lattices in ARC/INFO (Environmental Systems Research Institute, Inc., Redlands, CA) using the LATTICECONTOUR command to convert these lattices into contour maps. Hence, the 1 m contour map reproduced in Fig. 20–1b was created in two steps: (1) all 6,284 X,Y,Z values were used by ANUDEM to create a 10 m grid; and (2) this grid was brought into ARC/INFO as a lattice and used to create a detailed contour map.

Terrain Analysis

TAPES-G is a grid-based method of terrain analysis that calculates slope, aspect, specific catchment area, profile, plan and tangential curvature, and flow path length for each cell in a square-grid DEM (Moore, 1992). Specific catchment areas can be estimated using either the D8 algorithm that allows drainage from a node to only one of eight nearest neighbors based on the direction of steepest descent, the quasi-random Rho8 algorithm, or the FRho8 algorithm that permits drainage from a node to multiple nearest neighbors on a slope-weighted basis. The Rho8 algorithm produces more realistic flow networks and the FRho8 algorithm permits the modeling of flow dispersion in upland areas, which is important in areas with convex topography (Moore, 1992; Moore et al., 1993d). Other programs use TAPES-G outputs to compute the spatial distribution of net radiation and minimum/maximum temperatures in complex topography (SRAD), spatially distributed wetness indices based on either a steady-state or quasi-dynamic subsurface flow assumption (DYNWET or WET), and the spatial distribution of soil loss and erosion and deposition potential in a catchment (EROS) (Moore, 1992).

Three primary attributes (elevation, slope gradient, and specific catchment area) and one secondary attribute (steady-state wetness index) were computed for this study. Elevation was estimated on a 10 m grid spacing with ANUDEM. The maximum slope or gradient, β (in degrees) was computed with a finite-difference algorithm in TAPES-G from the directional derivatives by:

$$\beta = \arctan\left[(f_x^2 + f_y^2)^{0.5}\right] \quad (1)$$

Specific catchment area was calculated with the FRho8 algorithm that allows flow to be distributed to multiple nearest-neighbor nodes in upland areas above defined channels and uses the Rho8 or D8 algorithms below points of channel initiation. The points of channel initiation are designated (indirectly) by the user when they specify the maximum grading area in TAPES-G since this variable represents the minimum catchment area needed to initiate channel flow. A minimum drainage area of 20,000 m^2 (approximately 10% of the study area) was arbitrarily used to initiate channel flow in this study. The proportion of flow or upslope contributing area assigned to multiple downslope nearest neighbors

above these channels was determined on a slope weighted basis using methods similar to those proposed by Freeman (1991) and Quinn et al. (1991), so that the fraction of catchment area passed to neighbor i is given by:

$$F_i = \text{Max}(0, \text{Slope}_i^{1.1}) / \Sigma [\text{Max}(0, \text{Slope}_j^{1.1})] \quad (2)$$

where Slope is the slope from the current node to the nearest neighbor.

The compound topographic wetness index, $\ln(A_s/\tan\beta)$, has been used to characterize the spatial distribution of zones of surface saturation and soil water content in landscapes (e.g., O'Loughlin, 1986; Moore et al., 1988), to map forest soils (Skidmore et al., 1991), and to characterize the spatial variability of soil properties in a toposequence in Colorado (Moore et al., 1993a, 1993b). This particular version of the wetness index incorporates two important assumptions, that: (i) the gradient of the piezometric head, which dictates the direction of subsurface flow, is parallel to the gradient of the surface topography; and (ii) steady-state conditions apply, although Barling (1992) and Barling et al. (1994) recently proposed a quasi-dynamic version to overcome some of the limitations of this steady-state assumption.

The steady-state wetness index is used here to illustrate the effects of the number and pattern of elevation data on a hydrologically important compound topographic attribute. The value of this index increases with increasing specific catchment area and decreasing slope gradient, resulting in moderate values on hilltops (flat areas with low specific catchment area), high values in valleys (high specific catchment area and low slope) where water concentrates, and low values on steep hillslopes (high slope) where water drains more freely (Moore et al., 1993c).

Study Area and Evaluation Methods

The study area consists of a 20 ha (50 acre) farm field located at the base of the Bridger Mountains near the community of Springhill, Montana (T1N R6E, Section 8). It has a generally southerly aspect, moderately strong relief (43 m), and an average elevation of 1509 m (Fig. 20–1b and 20–1c). Minimum, maximum, and mean values for selected terrain indices are summarized in Table 20-1. A small intermittent stream runs through the field in a south-south-westerly direction (see bottom half of wire-mesh diagram). The soils are mostly fine-loamy Pachic and Udic Haploborolls and Agriborolls that have been farmed with a grain-fallow rotation for about 50 years.

Our primary goal was to determine how few GPS input data would be required to preserve key information about the computed terrain surfaces, since data collection, storage, and analysis may add additional costs to soil specific crop management applications. Elevation, slope gradient, specific catchment area, and the steady-state wetness index are treated as key information and the tests involve comparisons of various grids developed with partial GPS input data sets and the surfaces that were constructed from all 6,284 GPS data (Fig. 20–1a).

Table 20–1. Computed terrain indices, Springhill site, Montana.

	Minimum	Maximum	Mean
Slope (percent)	0.4	27.3	9.5
Specific catchment area (m^2 m^{-1})	10.0	886.0	222.4
Steady-state wetness index	5.7	15.4	8.5

Partial GPS data sets were chosen in ways that more or less matched those that a farm operator or consultant might have collected with a hand-held GPS receiver or a mobile receiver mounted on a vehicle.

GPS data sets that a farmer might have collected with a hand-held GPS receiver were obtained by dividing the field into 25 m, 50 m, and 100 m grid cells and randomly selecting a pre-determined number of X,Y,Z values in each grid cell (Table 20–2). This approach is equivalent to a stratified random areal sample design (Berry & Baker, 1968), although the random element disappears fairly quickly as more data are selected and the sample begins to mimic the routes travelled by the pickup truck and mobile GPS receiver (compare Fig. 20–2a, 20–2b, 20–2c, and 20–2d with Fig. 20–1a). This discovery may not be very important (practical) given that most people would switch from a hand-held receiver to one mounted on a truck if their goal was to collect > 200 sets of X,Y,Z data, although some of these data sets were retained for this study and used to demonstrate the impact of pattern on computed topographic attributes.

GPS data sets that a farmer might have collected with a truck-mounted GPS receiver were obtained from selected north-south and west-east truck routes in order to examine the impact of the number and pattern of GPS data on computed topographic attributes. A total of six data sets were compiled in this way. Three data sets were contructed by choosing every second north-south and/or west-east truck route and three data sets were constructed by choosing all north-south and/or west-east truck routes. The turns at the end of the truck routes were omitted from all six data sets. Figure 20–3 shows the pattern of GPS data sets and resulting contour maps with 1 m contour intervals. Between 1,120 and 4,817 X,Y,Z data sets were chosen with these options.

Each of the seventeen irregular X,Y,Z data sets was converted into regular 10 m grids with ANUDEM. The drainage enforcement option was used in ANUDEM to maintain fidelity with the stream network that was identified by the software itself. The resulting regular grids were transferred to TAPES-G to compute topographic attributes and to ARC/INFO to perform the statistical analysis and create the 1 m contour maps reproduced in Fig. 20–1 through 20–3. The TAPES-G attributes were also transferred to the GRID module in ARC/INFO where most of the statistical analysis was performed.

The elevation, slope gradient, specific catchment area, and steady-state wetness index surfaces (grids) were compared with equivalent surfaces developed from all the GPS data to evaluate the impact of the number and pattern of GPS data on computed topographic attributes. The contour maps in Figs. 20–1b, 20–2, and 20–3 allow visual comparisons and the statistics in Tables 20–3 and

Table 20–2. GPS data sets g
simulating data from a hand-hel

Grid size (m)	No. of points selected	M
100 m	1	
100 m	2	
100 m	4	
50 m	1	
50 m	2	
50 m	4	
50 m	16	
25 m	1	
25 m	4	

20–4 provide additional details.

Mean absolute differenc
negative numbers. The root m
summarize the differences in va
and the Moran Index is used t
differences in topographic attri
differences and RMSE values i
grids and the grid constructed
Index values near zero indicate t
values approaching +1 indicat
differences are clustered). Th
assumption: that the closer th
generated with the full GPS da
data set that is being assessed
measures match those used by
existing methods for building tr
gridded digital elevation model

Figure 20–1b shows the
ARC/INFO, and all 6,284 GP
evident in this map and the acc
(Fig. 20–1c): (i) the hilltop mar
is flanked by gentle side slopes
to the east; (ii) the shallow dr
south-south-westerly direction
and (iii) the hilltop located in t

pringhill site, Montana.

	Maximum	Mean
	27.3	9.5
	886.0	222.4
	15.4	8.5

s that more or less matched those that
ve collected with a hand-held GPS
a vehicle.
have collected with a hand-held GPS
eld into 25 m, 50 m, and 100 m grid
ined number of X,Y,Z values in each
equivalent to a stratified random areal
nough the random element disappears
and the sample begins to mimic the
mobile GPS receiver (compare Fig.
. 20–1a). This discovery may not be
people would switch from a hand-held
eir goal was to collect > 200 sets of
sets were retained for this study and
on computed topographic attributes.
have collected with a truck-mounted
north-south and west-east truck routes
number and pattern of GPS data on
of six data sets were compiled in this
y choosing every second north-south
sets were constructed by choosing all
. The turns at the end of the truck
s. Figure 20–3 shows the pattern of
with 1 m contour intervals. Between
sen with these options.
X,Y,Z data sets was converted into
lrainage enforcement option was used
stream network that was identified by
grids were transferred to TAPES-G to
ARC/INFO to perform the statistical
eproduced in Fig. 20–1 through 20–3.
nsferred to the GRID module in
nalysis was performed.
ific catchment area, and steady-state
ed with equivalent surfaces developed
act of the number and pattern of GPS
The contour maps in Figs. 20–1b,
and the statistics in Tables 20–3 and

Table 20–2. GPS data sets generated with stratified random areal sample simulating data from a hand-held GPS receiver.

Grid size (m)	No. of points selected	Max. desired no. of points	No. of points actually selected
100 m	1	32	29
100 m	2	64	58
100 m	4	128	116
50 m	1	120	111
50 m	2	240	221
50 m	4	480	441
50 m	16	1920	1747
25 m	1	435	391
25 m	4	1740	1535

20–4 provide additional details.

Mean absolute differences are reported to avoid the offset of positive and negative numbers. The root mean square error (RMSE) is commonly used to summarize the differences in values between two or more grids in GIS packages, and the Moran Index is used to measure how clustered or how randomly the differences in topographic attributes distribute spatially. Large mean absolute differences and RMSE values indicate large discrepancies between the sample grids and the grid constructed with all 6,284 GPS data points, whereas Moran Index values near zero indicate that the differences were randomly distibuted and values approaching +1 indicate positive spatial autocorrelation (i.e., that the differences are clustered). This approach relies on an implicit but important assumption: that the closer the sample surface is to the equivalent surface generated with the full GPS data set, the better the performance of the sample data set that is being assessed. This assumption and the resultant statistical measures match those used by Lee (1991) in his pioneering work comparing existing methods for building triangular irregular network models of terrain from gridded digital elevation models.

RESULTS

Figure 20–1b shows the contour map that was produced with ANUDEM, ARC/INFO, and all 6,284 GPS data points. Three topographic features are evident in this map and the accompanying three-dimensional wire mesh diagram (Fig. 20–1c): (i) the hilltop marking the northern boundary of the study area that is flanked by gentle side slopes to the west and south and very steep side slopes to the east; (ii) the shallow drainage (valley) that traverses the study area in a south-south-westerly direction in the bottom (southern) half of the study area; and (iii) the hilltop located in the southeast quadrant whose northern side slopes

mark the southern margin of the valley identified as (ii). These topographic features were also observed in the field and they are used along with the statistical analysis of the differences in computed topographic attributes to assess the effectiveness of the different sample data sets.

Figures 20–2 and 20–3 show the GPS points that were actually selected and used to compute the topographic attributes as well as the contour maps that were produced with ANUDEM and ARC/INFO. The GPS points are so close together that they appear as lines in the left half of the figures. The contour maps were clipped to minimize edge effects and as a result, they cover a smaller portion of the study area than the GPS maps. The first three pairs of maps in Fig. 20–2 demonstrate the effect of selecting additional random points within 100 m grid cells. The first contour map was generated with only 29 GPS points and does not adequately delineate the western side slopes for the hilltop along the northern boundary nor the valley that traverses the southern half of the study area (Fig. 20–2a). Doubling the number of points selected in each grid cell (Fig. 20–2b) and doubling the number again (Fig. 20–2c) improved the delineation of the two hilltops and the valley. The third contour map is much better than the second map in defining the channel, in part because of the presence of a spurious pit near the southwest corner of the field in the second map (Fig. 20–2b). The contour map in Fig. 20–2d was produced when one X,Y,Z data point was chosen randomly from each 50 m cell. Both the total number of points selected (120 versus 128) and the resultant contour map are very similar to the best result that was achieved with 100 m cells (Fig. 20–2c). Finally, a comparison of these last two contour maps with the map produced from all 6,284 X,Y,Z data points indicates how few data were needed to generate a "reasonable" contour map of this particular field.

The contour maps produced with the linear samples tell a much different story. The first two contour maps reproduced in Fig. 20–3 were derived from the gridded DEMs that used every second and all of the north-south routes. Both contour maps show the major topographic features, although the second map captures much more of the fine-scale detail (Fig. 20–3a and 20–3b). The two contour maps derived from west-east sample data do much better in the northern half of the study area than they do in the southern half (compare Fig. 20–3c and 20–3d with Fig. 20–1b, and note the presence of spurious pits in the channel on both maps). This result was probably caused by the orientation of the truck routes relative to the channel and it illustrates the sensitivity of the surfaces produced with the orientation of the linear routes used to collect GPS data relative to the orientation of major topographic features (i.e., ridge and stream lines). The selection of every second north-south and west-east route captured 2,483 X,Y,Z data points (40% of the total points) and not surprisingly, this method produced a very similar contour map to the that produced with the full GPS data set (Fig. 20–3e).

Seventeen sets of elevation differences were computed by comparing the 11 grids from the stratified random area samples and the six grids computed from the linear samples with the grid generated with all 6,284 sets of X,Y,Z data. The 10 m by 10 m grid measured 63 rows by 24 columns, so that the total number of points is 1,512. A modest improvement in the fitted surface was achieved

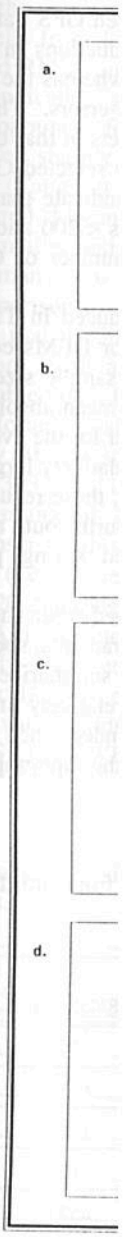

Fig. 20–2. GPS data sets
per 100 m cell (a), 2 po
and 1 point per 50 m ce

tified as (ii). These topographic
d they are used along with the
ed topographic attributes to assess
sets.
points that were actually selected
s as well as the contour maps that
FO. The GPS points are so close
half of the figures. The contour
ıd as a result, they cover a smaller
The first three pairs of maps in
ldditional random points within 100
ated with only 29 GPS points and
e slopes for the hilltop along the
es the southern half of the study
ınts selected in each grid cell (Fig.
0–2c) improved the delineation of
ıtour map is much better than the
:ause of the presence of a spurious
ıe second map (Fig. 20–2b). The
one X,Y,Z data point was chosen
ıl number of points selected (120
very similar to the best result that
Finally, a comparison of these last
'om all 6,284 X,Y,Z data points
ıte a "reasonable" contour map of

ıear samples tell a much different
l in Fig. 20–3 were derived from
nd all of the north-south routes.
hic features, although the second
ail (Fig. 20–3a and 20–3b). The
mple data do much better in the
ı the southern half (compare Fig.
ıe presence of spurious pits in the
ably caused by the orientation of
t illustrates the sensitivity of the
linear routes used to collect GPS
)graphic features (i.e., ridge and
north-south and west-east route
total points) and not surprisingly,
nap to the that produced with the

were computed by comparing the
ples and the six grids computed
ted with all 6,284 sets of X,Y,Z
's by 24 columns, so that the total
ıt in the fitted surface was achieved

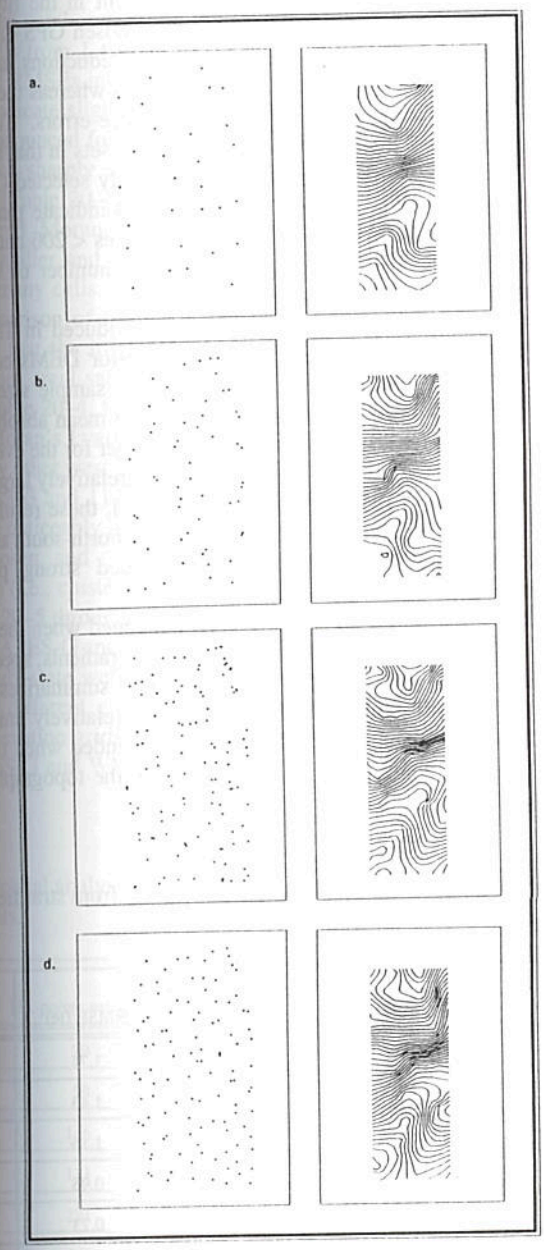

Fig. 20–2. GPS data sets and 1 m contour maps produced with 1 sample point per 100 m cell (a), 2 points per 100 m cell (b), 4 points per 100 m cell (c), and 1 point per 50 m cell (d).

number of points is 1,512. A modest improvement in the fitted surface was achieved by increasing the number of randomly chosen GPS data points in the 100 m grid cells from 1 to 4 (Table 20–3). The reductions in mean absolute differences and RMSEs indicate smaller differences whereas the declines in the Moran index indicate slightly less clustering of these errors. These trends are much more pronounced for the 25 m and 50 m data sets in that the values of all three indices fell sharply as the number of randomly selected GPS data points was increased (Table 20–3). Overall, these results indicate that the errors are strongly clustered (Moran's I > 0.60) for sample sizes < 200 and that the errors are typically smaller and less clustered if a small number of GPS points are selected from many cells.

A comparison of the statistical results reproduced in Tables 20–3 and 20–4 confirms that the linear paths produced inferior DEMs compared to the stratified random areal samples for roughly similar sample sizes. The results presented in Table 20–4, for example, show that the mean absolute differences, RMSEs, and Moran's I values were consistently larger for the every other north-south and every other west-east samples despite the relatively large sizes of these samples (n = 1363 and 1120, respectively). Overall, these results indicate that the errors were noticeably larger when every second north-south and/or west-east route was chosen and that these errors exhibited strong positive spatial autocorrelation (i.e., clustering).

Tables 20–5 through 20–7 show what happened when the elevation data were used in TAPES-G and WET to calculate slope gradients, specific catchment areas, and steady-state wetness indices. Table 20–5 summarizes the arithmetic means for the different grids and shows how the relatively small differences between the elevation grids (< 0.05%) were compounded when these data were input to TAPES-G and WET and used to calculate the topographic attributes.

Table 20–3. Spatial analysis of elevation differences from stratified random area sample points.

Grid size	No. points selected	Mean absolute elev. diff. (m)	RMSE (m)	Moran's Index
100/1	29	1.39	1.71	0.89
100/2	58	1.04	1.43	0.86
100/4	116	0.78	1.16	0.81
50/1	111	0.60	0.95	0.74
50/2	221	0.43	0.73	0.58
50/4	441	0.31	0.60	0.46
50/16	1747	0.16	0.40	0.19
25/1	391	0.27	0.54	0.39
25/4	1535	0.16	0.40	0.19

vement in the fitted surface was
ly chosen GPS data points in the
The reductions in mean absolute
ences whereas the declines in the
f these errors. These trends are
data sets in that the values of all
ndomly selected GPS data points
esults indicate that the errors are
le sizes < 200 and that the errors
small number of GPS points are

reproduced in Tables 20–3 and
inferior DEMs compared to the
imilar sample sizes. The results
at the mean absolute differences,
y larger for the every other north-
the relatively large sizes of these
)verall, these results indicate that
cond north-south and/or west-east
xhibited strong positive spatial

appened when the elevation data
lope gradients, specific catchment
20–5 summarizes the arithmetic
the relatively small differences
ompounded when these data were
ulate the topographic attributes.

ences from stratified random area

	RMSE (m)	Moran's Index
	1.71	0.89
	1.43	0.86
	1.16	0.81
	0.95	0.74
	0.73	0.58
	0.60	0.46
	0.40	0.19
	0.54	0.39
	0.40	0.19

by increasing the number of randomly chosen GPS data points in the 100 m grid 100 m grid cells from 1 to 4 (Table 20–3). The reductions in mean absolute differences and RMSEs indicate smaller differences whereas the declines in the Moran index indicate slightly less clustering of these errors. These trends are much more pronounced for the 25 m and 50 m data sets in that the values of all three indices fell sharply as the number of randomly selected GPS data points was increased (Table 20–3). Overall, these results indicate that the errors are strongly clustered (Moran's I > 0.60) for sample sizes < 200 and that the errors are typically smaller and less clustered if a small number of GPS points are selected from many cells.

A comparison of the statistical results reproduced in Tables 20–3 and 20–4 confirms that the linear paths produced inferior DEMs compared to the stratified random areal samples for roughly similar sample sizes. The results presented in Table 20–4, for example, show that the mean absolute differences, RMSEs, and Moran's I values were consistently larger for the every other north-south and every other west-east samples despite the relatively large sizes of these samples (n = 1363 and 1120, respectively). Overall, these results indicate that the errors were noticeably larger when every second north-south and/or west-east route was chosen and that these errors exhibited strong positive spatial autocorrelation (i.e., clustering).

Tables 20–5 through 20–7 show what happened when the elevation data were used in TAPES-G and WET to calculate slope gradients, specific catchment areas, and steady-state wetness indices. Table 20–5 summarizes the arithmetic means for the different grids and shows how the relatively small differences between the elevation grids (< 0.05%) were compounded when these data were input to TAPES-G and WET and used to calculate the topographic attributes.

Table 20–3. Spatial analysis of elevation differences from stratified random area sample points.

Grid size	No. points selected	Mean absolute elev. diff. (m)	RMSE (m)	Moran's Index
100/1	29	1.39	1.71	0.89
100/2	58	1.04	1.43	0.86
100/4	116	0.78	1.16	0.81
50/1	111	0.60	0.95	0.74
50/2	221	0.43	0.73	0.58
50/4	441	0.31	0.60	0.46
50/16	1747	0.16	0.40	0.19
25/1	391	0.27	0.54	0.39
25/4	1535	0.16	0.40	0.19

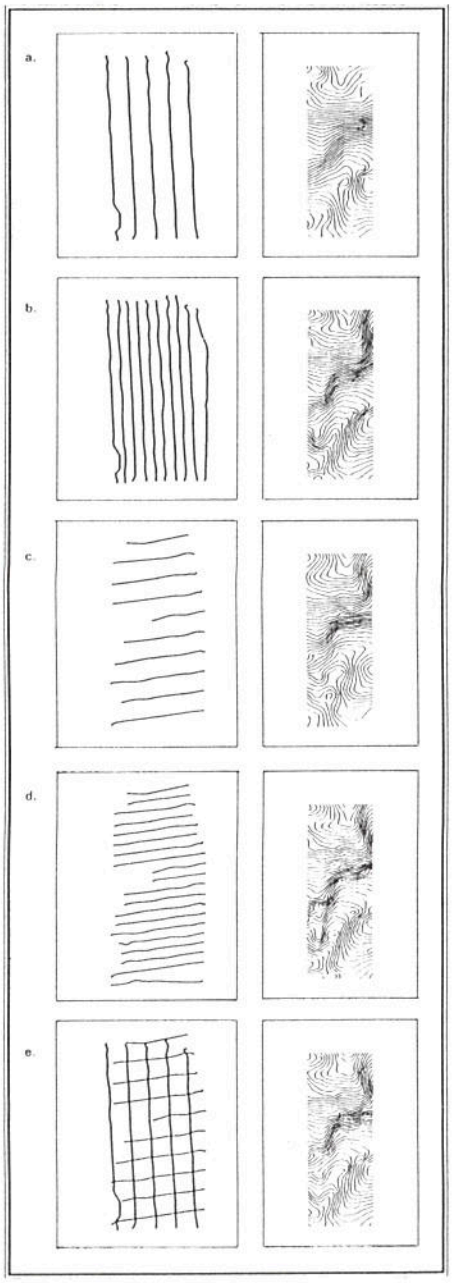

Fig. 20–3. GPS data sets and 1 m contour maps produced with every second north-south truck route (a), every north-south route (b), every second west-east route (c), every west-east route (d), and every second north-south and west-east truck route (e).

Table 20–4. Spatia
simulating dat

Linear routes	No. poin
0-1-0 NS	1
All NS	2
0-1-0 WE	1
All WE	2
0-1-0 NSWE	2
All NSWE	4

Table 20–5. Arithmet

Sample	Elevati
100/1	150
100/2	150
100/4	150
50/1	150
50/2	150
50/4	150
50/16	150
25.1	150
25/4	150
0-1-0 NS	150
All NS	1509
0-1-0 WE	1509
All WE	1509
0-1-0 NSWE	1509
All NSWE	1509
All data	1509

maps produced with every second
ath route (b), every second west-east
very second north-south and west-

Table 20–4. Spatial analysis of elevation differences from linear routes simulating data from a truck-mounted receiver.

Linear routes	No. points selected	Mean absolute elev. diff. (m)	RMSE (m)	Moran's Index
0-1-0 NS	1363	0.35	1.20	0.81
All NS	2682	0.21	0.51	0.42
0-1-0 WE	1120	0.62	0.96	0.72
All WE	2135	0.22	0.48	0.34
0-1-0 NSWE	2483	0.35	0.66	0.60
All NSWE	4817	0.05	0.23	0.11

Table 20–5. Arithmetic means for selected topographic attributes.

Sample	Elevation (m)	Slope gradient (percent)	Specific catchment. area (m^2 m^{-1})	Wetness Index
100/1	1508.4	7.1	306.9	7.53
100/2	1508.9	7.6	263.5	7.33
100/4	1508.9	8.3	297.8	7.12
50/1	1509.0	8.6	238.8	7.09
50/2	1509.0	9.4	234.8	6.93
50/4	1509.0	9.9	243.5	6.78
50/16	1509.1	11.1	242.6	6.63
25.1	1509.1	9.9	238.8	6.79
25/4	1509.1	11.1	243.7	6.62
0-1-0 NS	1509.1	8.3	353.3	7.20
All NS	1509.0	10.0	240.2	6.77
0-1-0 WE	1509.2	9.1	281.2	6.95
All WE	1509.1	10.5	271.3	6.70
0-1-0 NSWE	1509.1	9.8	282.6	6.81
All NSWE	1509.1	10.8	255.9	6.67
All data	1509.1	9.5	222.5	6.76

Table 20–6. Spatial analysis of topographic attribute differences from stratified random samples.

Sample	Slope gradient			Specific catchment area			Wetness index		
	MAD	RMSE	Moran	MAD	RMSE	Moran	MAD	RMSE	Moran
100/1	3.48	4.14	0.78	333.6	1381.5	0.05	1.30	1.51	0.64
100/2	3.18	3.85	0.76	294.3	1262.2	0.05	1.13	1.44	0.64
100/4	2.68	3.54	0.72	299.5	1399.8	0.07	0.97	1.35	0.55
50/1	2.37	3.06	0.65	227.2	1041.9	0.01	0.83	1.17	0.49
50/2	2.03	2.72	0.57	234.6	1109.7	-0.09	0.71	1.11	0.37
50/4	1.97	2.65	0.53	131.2	738.6	-0.11	0.54	0.87	0.33
50/16	2.02	2.46	0.36	103.7	747.1	0.01	0.39	0.64	0.09
25/1	1.82	2.47	0.49	172.3	909.3	-0.12	0.55	0.90	0.24
25/4	2.06	2.42	0.35	98.6	694.9	0.07	0.41	0.65	0.16

The results summarized in Table 20–6 show how the size and pattern of the errors for the primary and secondary topographic attributes varied with the different stratified random area samples. The magnitude and clustering of the slope gradient errors decreased gradually as the cells decreased in size (i.e., the spread improved) and sample size was increased. The mean slope gradients for the sample grids ranged from 75% to 117% of the mean slope gradient (9.5 degrees) on the grid computed with the entire X,Y,Z GPS data set (Table 20–5). The specific catchment area means for the sample grids are all larger than that for the complete GPS data set and confirm that the sample elevation grids missed some of the fine-scale topographic variation (Table 20–5). The mean absolute differences (MADs) and RMSEs reported in Table 20–6 confirm this trend and indicate that there were substantial reductions in the magnitude of these errors as the number and spread of the sample data was increased. The spatial pattern of these errors was more or less random for all of the samples (as would be expected for a variable that accumulates flow from upslope cells). The relative magnitude and clustering of the steady-state wetness index errors expressed as percentages fell between those of the two primary attributes from which this compound index is calculated. The magnitude and level of clustering of the wetness index errors decreased as sample size and spread increased (Table 20–6).

Similar results were obtained with the linear samples, so that: (i) the magnitude and clustering of errors decreased as the number of truck routes was increased for slope gradient and the steady-state wetness index, and (ii) the magnitude of the errors decreased for specific catchment area although these errors were randomly distributed (Table 20–7).

Table 20–7. Spatial analysis
samples.

Sample	Slope gradient		
	MAD	RMSE	Moran
0-1-0 NS	2.69	3.79	0.76
All NS	1.67	2.31	0.47
0-1-0 WE	2.48	3.28	0.68
All WE	1.79	2.27	0.45
0-1-0 NSWE	2.01	2.78	0.57
All NSWE	1.62	1.97	0.32

GPS technology is increa
method for collecting the irregu
inputs to construct digital elevat
terrain attributes. The grid surfa
sets were compared with the su
6,284 GPS-derived X,Y,Z points
graphically as elevation contou
elevation, slope gradient, specifi
were used to summarize the perf

These statistical comparis
input data will influence the DE
particular, they show that: (i)
distribution of these errors dimin
and clustering of the errors dimi
and (iii) that seemingly small
differences in the computed prin
last observation has important i
spatially-variable attributes to pr
1989; Moore et al., 1993a, 1993
non-point source pollution and otl
et al., 1991). Researchers, fa
technology in order to build DEM
of these differences and should o

ute differences from stratified

area	Wetness index		
Moran	MAD	RMSE	Moran
0.05	1.30	1.51	0.64
0.05	1.13	1.44	0.64
0.07	0.97	1.35	0.55
0.01	0.83	1.17	0.49
-0.09	0.71	1.11	0.37
-0.11	0.54	0.87	0.33
0.01	0.39	0.64	0.09
-0.12	0.55	0.90	0.24
0.07	0.41	0.65	0.16

w how the size and pattern of phic attributes varied with the agnitude and clustering of the ells decreased in size (i.e., the The mean slope gradients for the mean slope gradient (9.5 Y,Z GPS data set (Table 20–5). grids are all larger than that for sample elevation grids missed ble 20–5). The mean absolute le 20–6 confirm this trend and he magnitude of these errors as creased. The spatial pattern of samples (as would be expected cells). The relative magnitude errors expressed as percentages om which this compound index ing of the wetness index errors able 20–6).

inear samples, so that: (i) the the number of truck routes was ite wetness index, and (ii) the hment area although these errors

Table 20–7. Spatial analysis of topographic attribute differences from linear samples.

Sample	Slope gradient			Specific catchment area			Wetness index		
	MAD	RMSE	Moran	MAD	RMSE	Moran	MAD	RMSE	Moran
0-1-0 NS	2.69	3.79	0.76	347.5	1443.8	0.14	0.99	1.42	0.58
All NS	1.67	2.31	0.47	163.4	941.0	-0.03	0.49	0.84	0.23
0-1-0 WE	2.48	3.28	0.68	259.8	1248.1	0.08	0.73	1.17	0.41
All WE	1.79	2.27	0.45	143.8	891.2	0.10	0.44	0.77	0.22
0-1-0 NSWE	2.01	2.78	0.57	242.7	1228.0	0.15	0.61	1.08	0.34
All NSWE	1.62	1.97	0.32	102.1	789.3	0.10	0.32	0.63	0.13

CONCLUSIONS

GPS technology is increasingly advocated as a cost-effective and accurate method for collecting the irregularly-spaced elevation data that are required as inputs to construct digital elevation models and compute primary and secondary terrain attributes. The grid surfaces generated from the 17 different sample data sets were compared with the surface developed with a DEM computed from all 6,284 GPS-derived X,Y,Z points in this study. Some of the results were shown graphically as elevation contours and spatial analyses of the differences in elevation, slope gradient, specific catchment area, and steady-state wetness index were used to summarize the performance of the different samples.

These statistical comparisons show that the number and pattern of the GPS input data will influence the DEM and terrain attributes that are computed. In particular, they show that: (i) the magnitude and clustering of the spatial distribution of these errors diminishes as sample size increases, (ii) the magnitude and clustering of the errors diminishes as the spread of the input data increases, and (iii) that seemingly small variations in elevation may result in large differences in the computed primary and secondary topographic attributes. This last observation has important implications for those who want to used these spatially-variable attributes to predict other environmental variables (e.g., Dikau, 1989; Moore et al., 1993a, 1993b) and those who want to use them as inputs to non-point source pollution and other kinds of environmental models (e.g., Panuska et al., 1991). Researchers, farmers, and consultants wanting to use GPS technology in order to build DEMs and perform terrain analysis should be aware of these differences and should organize their data collection efforts accordingly.

REFERENCES

Barling, R.D. 1992. Saturation zones and ephemeral gullies on arable land in southeastern Australia. Unpubl. Ph.D. dissert., Univ. of Melbourne, Melbourne, Australia. 339p.

Barling, R.D., I.D. Moore, and R.B. Grayson. 1994. A quasi-dynamic wetness index for characterizing the spatial distribution of zones of surface saturation and soil water content. Water Resour. Res. 30: in press.

Berry, B.J., and A.H. Baker. 1968. Geographic sampling. pp. 91–100. *In* B.J. Berry, et al. (ed.) Spatial analysis: A reader in statistical geography. Englewood Cliffs, NJ. Prentice-Hall.

Bouma, J., and P.A. Finke. 1993. Origin and nature of soil resource variability. pp. 3–13. *In* P.C. Robert, et al. (ed.) Soil Specific Crop Management. Madison, WI. Soil Sci. Soc. Am.

Burrough, P.A. 1993. Soil variability: A late 20th century view. Soils and Fertilizers 56(5):529–565.

Dikau, R. 1989. The application of digital relief models to landform analysis in geomorphology. pp. 51–77. *In* J. Raper (ed.) Three-dimensional applications in geographic information systems. New York, NY. Taylor and Francis.

Fisher, P.F. 1991. Modelling soil map-unit inclusions by Monte Carlo simulation. Int. J. Geogr. Info. Systems 5(2):193–208.

Freeman, G.T. 1991. Calculating catchment area with divergent flow based on a regular grid. Comp. and Geosci. 17:413–422.

Hutchinson, M.F. 1989. A new procedure for gridding elevation and stream line data with automatic removal of spurious pits. J. Hydrol. 106:211–232.

Klingebiel, A.A., E.H. Horvath, D.G. Moore, and W.U. Reybold. 1987. Use of slope, aspect, and elevation maps derived from digital elevation model data in making soil surveys. pp. 77–90. *In* W.U. Reybold, et al. (ed.) Soil Survey Techniques. Madison, WI. SSSA Spec. Publ. No. 20.

Larson, W.C., and P.C. Robert. 1993. Farming by soil. pp. 103–112. *In* R. Lal, et al. (ed.) Soil Management for Sustainability. Ankeny, IA. Soil and Water Conservation Society.

Lee, J. 1991. Comparison of existing methods for building triangular irregular network models of terrain from grid digital elevation models. Int. J. Geogr. Info. Systems 5(3):267–285

Moore, I.D. 1992. Terrain Analysis Programs for the Environmental Sciences: TAPES. Agric. Systems Info. Tech. 4(2):37–39.

Moore, I.D., G.J. Burch, and D.H. McKenzie. 1988. Topographic effects on the distribution of surface water and the location of ephemeral gullies. Trans. ASAE. 31:1383–1395.

Moore, I.D., P.E. Gessler, G.A. Nielsen, and G.A. Peterson. 1993a. Terrain analysis for soil specific crop management. pp. 27–56. *In* Robert, P.C., et al. (ed) Soil Specific Crop Management. SSSA. Madison, WI.

Moore, I.D., P.E. Gessler, G.A. Nielsen, and G.A. Peterson. 1993b. Soil attribute prediction using terrain analysis. SSSA J. 57:443–452.

Moore, I.D., R.B. Grayson, and A review of hydrological, g Hydrol. Proc. 5(1):3–30.

Moore, I.D., A. Lewis, and J.C. method and scale effects. Modelling Change in Envi Sons.

Moore, I.D., A.K. Turner, J.P. Wi and land surface-subsurfac M.F., et al. (ed.) Environ Oxford Univ. Press.

Mulla, D.J. 1991. Using geostati fertility. p. 336–345. *In* K Twenty-first Century. St.

Mulla, D.J. 1993. Mapping and crop yield. p. 15–26. *In* Management. SSSA. Mad

Odeh, I.O.A., D.J. Chittleborough soil-landfrom interrelationsl 49(1):1–32.

O'Loughlin, E.M. 1986. Predi catchments by topographic

Panuska, J.C., I.D. Moore, and L.A into the Agricultural Non-P Water Conserv. 46(1):59–6

Quinn, P., K. Bevin, P. Chevallie hillslope flow paths for d terrain models. Hydrol. Pr

Rawls, W.J., D.J. Brakensiek, an properties. Trans. ASAE.

Skidmore, A.K., P.J. Ryan, W. Da of an expert system to ma system. Int. J. Geogr. Infc

Tyler, D.A. 1993. Positioning te et al. (ed.) Soil Specific Cr

Wagenet, R.J., J. Bouma, and R.B of soil survey information i Mausbach, et al. (ed.) S Madison, WI. SSSA Spec

ES

phemeral gullies on arable land in
.D. dissert., Univ. of Melbourne,

. 1994. A quasi-dynamic wetness
distribution of zones of surface
er Resour. Res. 30: in press.
hic sampling. pp. 91–100. *In* B.J.
A reader in statistical geography.

d nature of soil resource variability.
.) Soil Specific Crop Management.

late 20th century view. Soils and

elief models to landform analysis in
J. Raper (ed.) Three-dimensional
n systems. New York, NY. Taylor

p-unit inclusions by Monte Carlo
ems 5(2):193–208.
nt area with divergent flow based on
17:413–422.
er gridding elevation and stream line
ious pits. J. Hydrol. 106:211–232.
e, and W.U. Reybold. 1987. Use of
ived from digital elevation model data
. *In* W.U. Reybold, et al. (ed.) Soil
SSSA Spec. Publ. No. 20.
ning by soil. pp. 103–112. *In* R. Lal,
ustainability. Ankeny, IA. Soil and

thods for building triangular irregular
digital elevation models. Int. J. Geogr.

grams for the Environmental Sciences:
. 4(2):37–39.
zie. 1988. Topographic effects on the
e location of ephemeral gullies. Trans.

and G.A. Peterson. 1993a. Terrain
gement. pp. 27–56. *In* Robert, P.C., et
ement. SSSA. Madison, WI.
nd G.A. Peterson. 1993b. Soil attribute
SSSA J. 57:443–452.

Moore, I.D., R.B. Grayson, and A.R. Ladson. 1991. Digital terrain modeling: A review of hydrological, geomorphological, and biological applications. Hydrol. Proc. 5(1):3–30.

Moore, I.D., A. Lewis, and J.C. Gallant. 1993c. Terrain attributes: Estimation method and scale effects. p. 30–38. *In* Jakeman, A.K., et al. (ed) Modelling Change in Environmental Systems. Chichester. John Wiley & Sons.

Moore, I.D., A.K. Turner, J.P. Wilson, S.K. Jenson, and L.E. Band. 1993d. GIS and land surface-subsurface process modeling. p. 196–230. *In* Goodchild, M.F., et al. (ed.) Environmental Modeling with GIS. New York, NY: Oxford Univ. Press.

Mulla, D.J. 1991. Using geostatistics and GIS to manage spatial patterns in soil fertility. p. 336–345. *In* Kranzler, G. (ed.) Automated agriculture in the Twenty-first Century. St. Joseph, MI. Am. Soc. Agric. Engr.

Mulla, D.J. 1993. Mapping and managing spatial patterns in soil fertility and crop yield. p. 15–26. *In* Robert, P.C., et al. (eds), Soil Specific Crop Management. SSSA. Madison, WI.

Odeh, I.O.A., D.J. Chittleborough, and A.B. McBratney. 1991. Elucidation of soil-landfrom interrelationships by canonical ordination analysis. Geoderma 49(1):1–32.

O'Loughlin, E.M. 1986. Prediction of surface saturation zones in natural catchments by topographic analysis. Water Resour. Res. 22(5):794–804.

Panuska, J.C., I.D. Moore, and L.A. Kramer. 1991. Terrain analysis: Integration into the Agricultural Non-Point Source (AGNPS) pollution model. J. Soil Water Conserv. 46(1):59–64.

Quinn, P., K. Bevin, P. Chevallier, and O. Planchon. 1991. The prediction of hillslope flow paths for distributed hydrological modeling using digital terrain models. Hydrol. Proc. 5(1):59–79.

Rawls, W.J., D.J. Brakensiek, and K.E. Saxton. 1982. Estimating soil water properties. Trans. ASAE. 25: 1316–1320, 1328.

Skidmore, A.K., P.J. Ryan, W. Dawes, D. Short, and E. O'Loughlin. 1991. Use of an expert system to map forest soils from a geographical information system. Int. J. Geogr. Info. Systems 5(4):431–445.

Tyler, D.A. 1993. Positioning technology (GPS). p. 159–165. *In* P.C. Robert, et al. (ed.) Soil Specific Crop Management. SSSA. Madison, WI.

Wagenet, R.J., J. Bouma, and R.B. Grossman. 1991. Minimum data sets for use of soil survey information in soil interpretive models. p. 161–182. *In* M.J. Mausbach, et al. (ed.) Spatial Variabilities of Soils and Landforms. Madison, WI. SSSA Spec. Public. No. 28.